A Thesis for the Degree of Master of Science

Molecular and Physiological Characterization of the Effect of *Ralstonia solanacearum* NLS-containing Type III Effectors on Immunity and Development in *Nicotiana benthamiana* and *Arabidopsis thaliana*

*Ralstonia solanacearum*의 NLS 이펙터가 애기장대와 담배의 면역과 발달에 미치는 분자생리적 영향 구명

FEBRUARY, 2019

HYELIM JEON

MAJOR IN HORTICULTURAL SCIENCE
AND BIOTECHNOLOGY
DEPARTMENT OF PLANT SCIENCE
THE GRADUATE SCHOOL OF
SEOUL NATIONAL UNIVERSITY

Molecular and Physiological Characterization of the Effect of *Ralstonia solanacearum* NLS-containing Type III Effectors on Immunity and Development in *Nicotiana benthamiana* and *Arabidopsis thaliana*

UNDER THE DIRECTION OF DR. CECILE SEGONZAC

SUBMITTED TO THE FACULTY OF THE GRADUATE SCHOOL
SEOUL NATIONAL UNIVERSITY

BY
HYELIM JEON

MAJOR IN HORTICULTURAL SCIENCE AND BIOTECHNOLOGY
DEPARTMENT OF PLANT SCIENCE
THE GRADUATE SCHOOL OF SEOUL NATIONAL UNIVERSITY

FEBRUARY, 2019

APPROVED AS A QUALIFIED THESIS OF HYELIM JEON
FOR THE DEGREE OF MASTER OF SCIENCE
BY THE COMMITTEE MEMBERS

CHAIRMAN _____
Byoung-Cheorl Kang, Ph.D.

VICE-CHAIRMAN _____
Cecile Segonzac, Ph.D.

MEMBER _____
Jin Hoe Huh, Ph.D.

Molecular and Physiological Characterization of the Effect of *Ralstonia solanacearum* NLS-containing Type III Effectors on Immunity and Development in *Nicotiana benthamiana* and *Arabidopsis thaliana*

HYELIM JEON

DEPARTMENT OF PLANT SCIENCE
THE GRADUATE SCHOOL OF SEOUL NATIONAL UNIVERSITY

ABSTRACT

Ralstonia solanacearum is a soil-borne phytopathogen that causes lethal bacterial wilt in a wide range of food crops. Pathogenicity of *R. solanacearum* is mediated by the type III secretion system (T3SS) that injects type III effectors (T3Es) directly into host cells. T3Es are known to modulate not only plant immunity, but also various host cell processes for the bacterial infection. However, because of the complexity of *R. solanacearum* T3E repertoire, only few of them have been characterized for their mode of action. Here, I used heterologous expression of individual nuclear localization sequence (NLS)-containing *R. solanacearum* T3Es in *Nicotiana benthamiana* and *Arabidopsis thaliana* to screen the effectors that have effect on plant

immunity and development. Transient expression of the effectors in *N. benthamiana* revealed several effectors that induce cell death. Also, some of the candidate effectors disturbed reactive oxygen species (ROS) production and the subsequent induction of defense gene expression, which are early pattern-triggered immunity (PTI) responses. For stable expression of the effectors, effector-expressing *Arabidopsis* homozygous lines (EELs) were generated, and the ability of the effectors to interfere with PTI was examined. Finally, the effect of the effectors on *Arabidopsis* developmental processes was assessed in EELs, and one of the effectors, RipD, was shown to impair seed germination and root development. Selected effectors that target immune system and root development will be further characterized for their molecular targets and contribution to the pathogen virulence.

Key words: *Ralstonia solanacearum*, effectors, PTI, *Nicotiana benthamiana*, *Arabidopsis thaliana*, plant development

Student number: 2017-21031

CONTENTS

LIST OF TABLES

LIST OF FIGURES

LIST OF ABBREVIATIONS

ABA	Abscisic acid
BAK1	BRI1 ASSOCIATED KINASE1
CRN	Crinkler
das	day after sowing
dpi	day post-infiltration
EAR	Ethylene-responsive element binding factor-associated amphiphilic repression
EEL	Effector-expressing line
EFR	EF-Tu RECEPTOR
EF-Tu	Elongation factor Tu
ETI	Effector-triggered immunity
ETS	Effector-triggered susceptibility
fec	*fls2 efr cerk1* triple mutant
FL	Fluridone
FLS2	FLAGELLIN SENSING2
GA	Gibberellic acid
HR	Hypersensitive response
LD	Long-day
LR	Lateral root
MAPK	Mitogen-activated protein kinases
MS	Murashige and Skoog
NB-LRR	Nucleotide-binding leucine-rich repeat
NLS	Nuclear localization sequence

PAMP	Pathogen-associated molecular pattern
PR	Primary root
PRR	Pattern recognition receptors
PTI	PAMP-triggered immunity
Pto	*Pseudomonas syringae pv. tomato*
R gene	Resistance gene
RbohD	Respiratory burst oxidase homolog D
Rip	*Ralstonia* injected protein
RK	Receptor kinases
RLU	Relative light unit
ROS	Reactive oxygen species
RSSC	*Ralstonia solanacearum* species complex
SD	Short-day
T3E	Type III effector
T3SS	Type III secretion system
VIGS	Virus-induced gene silencing
WT	Wild-type
YFP	Yellow fluorescent protein

INTRODUCTION

Plants rely on a two-branched innate immune system to respond to infection (Jones and Dangl, 2006). The first branch uses transmembrane pattern recognition receptors (PRRs) that recognize conserved microbial elicitors called pathogen-associated molecular patterns (PAMPs). This recognition leads to PAMP-triggered immunity (PTI) in the host cell to restrict pathogen growth (Boller and Felix, 2009). Successful pathogens inject virulence molecules called effectors into plant cells to interfere with PTI and multiple host pathways, resulting in effector-triggered susceptibility (ETS). However, plants have evolved the second branch of immunity that specifically recognizes an effector via one of the intracellular nucleotide-binding leucine-rich repeat (NB-LRR) receptors encoded by resistance (R) genes. This effector-triggered immunity (ETI) induces amplified PTI response, resulting in disease resistance and often a form of programmed cell death at the infection site called hypersensitive response (HR).

PRRs are generally membrane-bound LRR receptor kinases (RKs). Upon PAMP perception, PRR forms stable heterodimers with certain co-receptors. This active receptor complex initiates intracellular signaling required for the defense responses. Most studies on PAMP perception were done in the model species *Arabidopsis thaliana*. In *Arabidopsis*, the RK FLAGELLIN SENSING2 (FLS2) recognizes the epitope flg22 of bacterial flagellin, which triggers formation of a receptor complex with the co-receptor BRI1 ASSOCIATED KINASE1

(BAK1) (Chinchilla et al., 2007; Heese et al., 2007). Similarly, elf18 of the bacterial elongation factor Tu (EF-Tu) is perceived by EF-Tu RECEPTOR (EFR), forming an active receptor complex with BAK1 (Kunze et al., 2004; Zipfel et al., 2006).

Activation of PRRs induces various defense signaling events. Within seconds after PAMP perception, there are changes in ion fluxes across the plasma membrane including an influx of Ca^{2+} from the apoplast (Blume et al., 2000; Lecourieux et al., 2006). This Ca^{2+} influx was shown to be essential for two distinct downstream signaling events, reactive oxygen species (ROS) production and activation of mitogen-activated protein kinases (MAPKs) leading to transcriptional changes (Segonzac et al., 2011; Kadota et al., 2015). In *Arabidopsis*, respiratory burst oxidase homolog D (RbohD) plays a key role in apoplastic ROS generation induced by PAMP perception (Torres et al., 2002; Nuhse et al., 2007; Zhang et al., 2007). This rapid and transient ROS production is thought to contribute to immunity in different ways: as direct antimicrobial agent, as cross-linking components to reinforce cell walls; and as secondary messengers during signal transduction (Torres, 2010; Segonzac et al., 2011). Another early event downstream of PAMP perception is activation of MAPK cascades. Successful signal transduction leads to defense-oriented transcriptional reprogramming, where the expression of approximately 10% of the whole plant transcriptome is altered (Navarro et al., 2004; Moore et al., 2011). This results in production of antimicrobial compounds and callose deposition at the cell wall.

The gram-negative bacterial species *Ralstonia solanacearum* is

a soil-borne phytopathogen that causes bacterial wilt disease (Peeters et al., 2013). Because of its devastating lethality and wide geographical distribution and host range, *R. solanacearum* is considered as one of the most important bacterial plant pathogens (Mansfield et al., 2012). It is a heterogeneous species with extensive diversity and therefore commonly called *R. solanacearum* species complex (RSSC) (Genin and Denny, 2012). The RSSC is classified into the four major monophyletic clusters of strains termed phylotypes that reflect their geographical origins. The pathogenicity of *R. solanacearum* relies on a type III secretion system (T3SS) which injects type III effector (T3E) proteins directly into plant cells (Genin, 2010). These T3Es, named Rips (*Ralstonia* injected proteins), are presumed to manipulate diverse host cell processes to favor infection (Poueymiro and Genin, 2009). Genomic analysis of the RSSC strains revealed 94 T3E orthologous groups and GMI1000, a reference strain in phylotype, contains 72 T3Es, which is exceptionally large number compared with other bacterial plant pathogens (Coll and Valls, 2013). This complexity of RSSC T3E repertoires and their redundant functions made it difficult to identify their molecular characteristics so that only few of them have been investigated so far. Most of the identified functions are related to the effect on the host immune system. The GALA family of effectors (RipG) carrying F-box domain in their leucine-rich repeats interferes with host ubiquitin pathway to inhibit PTI and promote disease (Angot et al., 2006). Another effector, RipAY, was also recently found to suppress PTI via exhibiting γ-glutamyl cyclotransferase activity to degrade glutathione that plays

important roles in the immune system (Fujiwara et al., 2016; Mukaihara et al., 2016; Sang et al., 2018).

Apparently, the major role of T3Es is the suppression of plant immunity as identified in numerous studies on T3Es with immuno-suppressive abilities over the years (Deslandes and Genin, 2014; Macho and Zipfel, 2015). However, multiple T3Es have been shown to target different cellular processes that are not directly related to immunity such as hormone signaling pathways, cell biology, and development. In some cases, these manipulations could result in indirect suppression of plant immunity to promote bacterial infection and proliferation (Macho, 2016). Elucidating how effectors target various non-immune cellular functions has furthered our understanding of plant biology, which makes effectors valuable molecular probes (Lee et al., 2013). For example, the findings that an effector from *Phytophthora infestans* called PexRD54 interacts with autophagy-related protein ATG8CL and that the effector competes with the host cargo receptor Joka2 helped understanding the nature of selective autophagy (Dagdas et al., 2016). Moreover, the *R. solanacearum* nuclear effector PopP2 (also called RipP2) was demonstrated to target WRKY transcription factors that are involved in defense transcriptional reprogramming (Le Roux et al., 2015; Sarris et al., 2015). For this PTI suppression, the presence of EAR (ethylene-responsive element binding factor-associated amphiphilic repression) motif in PopP2 was required (Segonzac et al., 2017). These findings not only provide a mechanism to manipulate plant genomes, but also highlight the biological relevance of nuclear localization of effectors.

Some effectors interfering with developmental processes induce morphological changes. The phytoplasma effector SAP11 binds transcription factors that control plant development (Sugio et al., 2011). *SAP11* transgenic *Arabidopsis* lines have crinkled leaves and a bushy appearance with more stems which may attract more insect vectors for phytoplasma. *R. solanacearum* also uses T3Es to alter root morphology (Lu et al., 2018). In vitro infection with *R. solanacearum* causes a triple phenotype on *Arabidopsis* root: root growth inhibition, root hair formation, and root tip cell death. Among these phenotypes, root hair production and cell death induction were proved to be T3SS-dependent. Also auxin signaling was required for the root hair phenotype. Considering the fact that *R. solanacearum* harbors auxin biosynthesis genes, it is possible that this root pathogen hijacks plant hormonal control to change root architecture and provide entry points for the bacteria (Valls et al., 2006).

In this study, *R. solanacearum* type III effectors predicted to be localized to the nucleus were used as molecular probes to decipher fundamental plant processes possibly manipulated by the pathogen. To this aim, individual effectors were expressed heterologously in two different model plants, *Arabidopsis* and *Nicotiana benthamiana* to screen out the effectors that can affect plant immune system and/or development. Via transient expression of the candidate effectors in *N. benthamiana* leaves, their ability to suppress PAMP-induced immune responses such as ROS burst and defense gene expression was tested. Additionally, this immuno-suppressive activity was analyzed again in *Arabidopsis* transgenic lines that stably express the effectors, named

EELs. Finally, abilities of the effectors to alter plant morphology or development were also assessed in EELs. The results were organized into three parts:

1. Characterization of the effect of *R. solanacearum* NLS-containing type III effectors on immunity following transient expression in *N. benthamiana*
2. Characterization of the effect of *R. solanacearum* NLS-containing type III effectors on immunity through constitutive expression in *Arabidopsis*
3. Preliminary morphological and physiological characterization of the EELs

This work is the first step to initiate the study to identify the effect of the *R. solanacearum* type III effectors on host cellular processes. Some of the candidate effectors were found to impair PTI responses in *N. benthamiana* or *Arabidopsis*, and others to disturb *Arabidopsis* development in different stages. Further examination of the selected effectors will help get insights into mechanisms relevant to the effector-induced phenotypes and better understand how *R. solanacearum* hijacks plant processes.

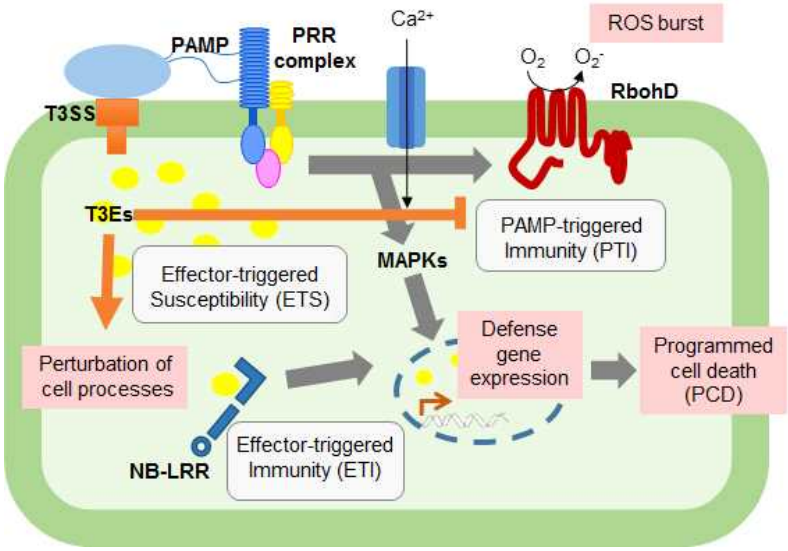

Figure 1. Plant immune system and cellular functions targeted by type III effectors

Plants perceive pathogen-associated molecular patterns (PAMPs) via extracellular pattern-recognition receptors (PRRs). This recognition induces PAMP-triggered immunity (PTI) responses including burst of Ca^{2+} and reactive oxygen species (ROS), activation of mitogen-acivated protein kinases (MAPKs), and induction of defense genes to restrict pathogen infection. To overcome PTI, successful bacterial pathogens use type III secretion system (T3SS) to inject effector proteins into the cells. These type III effectors (T3Es) manipulates plant immunity and various cellular processes to make favorable environment for the bacterial infection. Recognition of specific effectors by nucleotide-binding leucine-rich repeat (NB-LRR) receptors induces effector-triggered immunity (ETI), often leading to programmed cell death called hypersensitive response (HR).

MATERIALS AND METHODS

Plant materials

Nicotiana benthamiana plants were grown in a growth chamber at 24 to 26°C and 60% relative humidity under 16 h light/8 h dark cycle. Seeds of *Arabidopsis thaliana* wild-type (WT) Columbia (Col-0), *fls2*, and *fls2 efr cerk1* triple mutants were provided from Plant immunity laboratory at Pohang University of Science and Technology (POSTECH). *Arabidopsis* plants were grown in a growth chamber at 23°C and 60% relative humidity under 16 h/8 h or 10 h/14 h cycle for long-day (LD) or short-day (SD) condition, respectively.

To generate transgenic effector-expressing line, Col-0 plants were transformed with *Agrobacterium tumefaciens* strain AGL1 carrying *35S::Rip-3xFLAG* constructs using floral dip method (with Dr. Wanhui Kim). Primary transformants (T1) seeds were screened on Murashige and Skoog (MS) medium containing kanamycin as selective antibiotic. T2 seeds descending from self-pollination of T1 plants were screened on the same medium and the T2 seedlings following 3:1 (recovered: dead) segregation ratio were selected. Verified T3 homozygous lines descending from self-pollination of the selected T2 plants were used for further analysis.

Construction of *Ralstonia solanacearum* NLS-containing effector library

E. Coli DH5α clones carrying entry modules for each selected NLS-containing effector were provided from Plant immunity laboratory

at POSTECH. The entry modules were assembled in fusion with 3xFLAG under the control of the cauliflower mosaic virus (CaMV) 35S promoter in the binary vector pICH86988 using Golden Gate cloning (with Dr. Wanhui Kim). Assemblies confirmed by restriction analysis were mobilized into *A. tumefaciens* AGL1 strain and stored as cell stock at -80°C.

A. tumefaciens-mediated transient expression assays

For transient effector expression in *N. benthamiana, A. tumefaciens* AGL1 cells containing the respective effector and GFP construct were resuspended in infiltration medium (10 mM $MgCl_2$ and 10 mM MES-KOH, pH=5.6) to reach OD_{600} = 0.5. This solution was infiltrated in fully expanded leaves of 5-6 week-old plants.

Ion leakage assay

N. benthamiana leaf discs expressing *GFP* and each effector were collected using 8 mm diameter cork borer just after infiltration and at 3 days post-infiltration (dpi). The leaf discs were shaken in 12-well tissue culture plates with 2 ml of demineralized water for 2 hours at 150 rpm. Then water conductivity in each well was measured using a Horiba B-771 LAQUAtwin compact conductivity meter (Horiba).

Measurement of ROS production

Leaf discs of *N. benthamiana* or *Arabidopsis* grown under SD condition were collected using 5 mm diameter biopsy punch. The leaf discs were floated on 150 μl of demineralized water overnight and

ROS released by the leaf discs were measured using a chemiluminescent assay. The water was replaced with 100 μl of assay solution containing 100 μM luminol (Sigma-Aldrich) and 2 μg of horseradish peroxydase (Sigma-Aldrich). ROS was elicited with 100 nM flg22 (Peptron) in *N. benthamiana* or 100 nM and 10 nM flg22 or elf18 (Peptron) in *Arabidopsis*. Luminescence was measured in relative light unit (RLU) over a time period of 75 min using GloMax 96 Microplate Luminometer (Promega).

RT-PCR

N. benthamiana leaf discs expressing *GFP* and each effector were collected at 1 dpi, and floated on water overnight. Then the leaf discs were treated with water or 100 nM flg22 for 60 min and frozen in liquid nitrogen. Total RNA was extracted using TRIzol-Reagent (Ambion) and treated with DNase I (Sigma-Aldrich). First-strand cDNA was synthesized from 2.5 μg of RNA using Maxima first strand cDNA synthesis kit (Thermo scientific). For quantitative RT-PCR, 4 μl of diluted cDNA was combined with GoTaq qPCR master mix (Promega) and then PCRs were performed with three technical repeats. Expression of defense marker genes was normalized by *NbEF1α* expression.

RNA extraction and cDNA synthesis from *Arabidopsis* leaf discs were performed in the same way. RT-PCR analysis was carried out with cDNA derived from leaves of WT and T3 homozygous lines using each effector specific primer set. *AtEF1α* was amplified as an internal control. The sequence of primers used for the analysis is

listed in Table 1.

Elf18-triggered growth inhibition assay

Arabidopsis seeds were sterilized with 0.05% Triton X-100 (Sigma-Aldrich) and 70% ethanol twice followed by 95% ethanol once. Sterilized seeds were sown on half-strength MS containing 1% sucrose and 0.8% agar, and then grown for 5 under 16 h of light after 3 days of stratification at 4°C. Two 5-day-old seedlings were transferred to each well of 24-well tissue culture plates filled with 1 ml of liquid MS medium containing increasing concentration (0, 1, 10, 50 nM) of elf18. After grown in the liquid MS for 9 more days, fresh weight of seedlings was measured on precision scale.

Root growth assay

Sterilized seeds were sown on half-strength MS vertical plates containing 1.2% agar and 1% sucrose. The plates were kept in the dark for more than 3 days at 4°C for stratification and then incubated in a growth chamber at 20°C and 60% relative humidity under 16 h of light. After growth for 11 days, plant photographs were taken for analysis.

Seed germination assay

For the plate-based analysis, sterilized seeds and MS medium were prepared with the same way used for root growth assay. Stock solution of gibberellin (GA_3, Sigma-Aldrich) and fluridone (FL, Sigma-Aldrich) dissolved in ethanol were added to the MS medium to

make the final concentration of ethanol 0.05%. More than thirty seeds of Col-0 and each *RipD*-transgenic line were sown on MS plates containing different concentrations of GA_3 (10, 100 μM), FL (5, 10 μM) or just 0.05% ethanol as a control. After stratification for 3 days, the plants were grown in the same growth chamber as for root growth assay. Radicle emergence was scored every day. For the soil-based analysis, more than 30 seeds of Col-0 and each effector-expressing line were sown on soil. The plants were grown in a growth chamber at 23°C and 60% relative humidity under LD or SD condition. Green cotyledon emergence was scored every day.

Analysis of leaf development

Pictures of effector-expressing *Arabidopsis* transgenic plants and Col-0 grown on soil were taken every 2 days. The images were corrected using color thresholding in ImageJ for segmentation and detection of rosettes. The corrected images were analyzed to measure total leaf area and maximum rosette diameter using Rosette Tracker software (De Vylder et al., 2012).

Table 1. List of primers

Gene	Sequence (5'→3')
NbEF1α	F: AAGGTCCAGTATGCCTGGGTGCTTGAC
	R: AAGAATTCACAGGGACAGTTCCAATACCAC
NbCYP71D20	F: AAGGTCCACCGCACCATGTCCTTAGAG
	R: AAGAATTCCTTGCCCCTTGAGTACTTGC
NbACRE31	F: AAGGTCCCGTCTTCGTCGGATCTTCG
	R: AAGAATTCGGCCATCGTGATCTTGGTC
NbACRE132	F: AAGGTCCAGCGAAGTCTCTGAGGGTGA
	R: AAGAATTCCAATCCTAGCTCTGGCTCCTG
AtEF1α	F: CAGGCTGATTGTGCTGTTCTTA
	R: GTTGTATCCGACCTTCTTCAGG
RipA2	F: CAATATGACCGTCAACCAGCAT
	R: AGTTCTTGATGCCGACCTTGA
RipD	F: GGCTTAAACACATGGGCCTTAC
	R: TGCTCATGTATTGCAGGAGGTT
RipL	F: GTCGATTCCAATTTCCGGCG
	R: AGACCGTGCGTGATCTCAAG
RipAD	F: CGCGCAAGTTCCAGTACAAGT
	R: GGAGTCGTTGTTGATGATCAGG
RipAO	F: TACAGCATGCCGGAAATCTATG
	R: CCTTTCATTGTGGTAGCGGTTC

RESULTS

Characterization of the effect of *Ralstonia solanacearum* NLS-containing type III effectors on immunity following transient expression in *N. benthamiana*

Sequence analysis of *R. solanacearum* type III effectors to identify NLS-containing effectors

Effector localization to the nucleus seems to play the crucial role as a significant number effectors from different pathogens, including PopP2 from *R. solanacearum*, are targeted to the plant nucleus to interact with key host factors (Deslandes and Rivas, 2011; Le Roux et al., 2015; Sarris et al., 2015). To identify *R. solanacearum* type III effectors that may function in the nucleus, the protein sequences of 80 GMI1000 effectors were downloaded from the web database (http://iant.toulouse.inra.fr/T3E) and analyzed for the search of nuclear localization sequence (NLS) using two different softwares, NLStradamus (Nguyen Ba et al., 2009) and cNLS mapper (Kosugi et al., 2009). As a result, 19 effector sequences, which is about 25% of GMI1000 repertoire, were predicted to carry putative NLS. Among these effectors, 13 effectors which are less than 5 kb-long were selected for molecular cloning to simplify the cloning procedure.

For each selected effector, about 1 kb-long modules were amplified from *R. solanacearum* model strain GMI1000 with BsaI

site-flanking primers. Amplified fragments were ligated into the pICH41021 vector and confirmed by DNA sequencing. Using BsaI-based Golden Gate assembly, entry modules for each effector were assembled in fusion with 3xFLAG tag under the control of 35S promoter in the binary pICH86988 vector. Confirmed assemblies of 10 effectors were obtained and mobilized into *A. tumefaciens* AGL1 for the transient expression in this study (Table 2). The effectors were also fused with yellow fluorescent protein (YFP) tag to examine their subcellular localization (results from Dr. Wanhui Kim and Boyoung Kim).

Table 2. List of effectors with predicted NLS

Name	Gene ID[a]	Amino acid length	Predicted NLS[b]	Functional domain/motif or function[c]	Subcellular localization[d]
RipA1	GMI1000.RSc2139	1063	91-KPAPRRMRPPAAPGRKH-107		Cytoplasm
RipA2	GMI1000.RSc0099	1127	88-PKAP-91		
RipAB	GMI1000.RSc0876	174	112-GKKKKKR-118		Nucleus
RipAD	GMI1000.RSc1601	310	114-ARAKSGKK-121		Chloroplast
RipAF1	GMI1000.RSc0822	350	36-R-36, 34-PRRPKNRG-41	Putative ADP-ribosyltransferase	Nucleus, cytoplasm
RipAO	GMI1000.RSc0879	498	210-RPAPMRQAARPAPPPARAP-228		Nucleus
RipAY	GMI1000.RSc1022	416	27-RKKNGSPPRR-36	γ-glutamyl cyclotransferase	Nucleus, cytoplasm
RipD	GMI1000.RSc0304	643	184-PRRKPS-189		Golgi apparatus or mitocondria
RipE1	GMI1000.RSc3369	425	407-RRRARRA-413		No signal
RipL	GMI1000.RSc0193	1403	1385-RAQPSKSKGKGTKGKGKAK-1403	Pentatricopeptide Repeats	Lipid body

[a] From https://iant.toulouse.inra.fr/T3E and PRJEB8376

[b] From NLStradamus (www.moseslab.csb.utoronto.ca/NLStradamus) and cNLS mapper (http://nls-mapper.iab.keio.ac.jp)

[c] From InterProScan and CD server, enzymatic activity of RipAY has been confirmed (Fujiwara et al., 2016; Mukaihara et al., 2016).

[d] Expression of YFP-effector fusion protein in *N.benthamiana* (oberved by Dr. Wanhui Kim and Boyoung Kim)

Three of the selected effectors elicited cell death in *N. benthamiana*

Recognition of an effector by the plant immune system results in ETI, usually inducing a hypersensitive cell death response (HR) (Jones and Dangl, 2006). To investigate if the selected effectors are recognized, cell death assays were performed by *A. tumefaciens*-mediated transient expression of the effectors in *N. benthamiana.* Leaf tissue expressing *RipA1* or *RipE1* started to exhibit strong cell death within 2-3 dpi (days post-inoculation). RipAY induced cell death later at 4-5 dpi (Figure 2A).

In addition, the effector-induced cell death was quantified by ion leakage assay (Figure 2B). In *N. benthamiana* leaf expressing *RipA1* or *RipE1*, but not *RipAY*, ion leakage was significantly increased compared to *GFP*-expressing control leaf at 3 dpi. Taken together, 3 of the 10 selected effectors induced cell death at different dpi when expressed transiently in *N. benthamiana* leaves. This means possible recognition of the three effectors although it needs further confirmation to rule out the possibility of effector toxicity. Thus, seven effectors that did not induce cell death were further examined for the ability to suppress two different PAMP-triggered immune responses, ROS burst and defense gene expression.

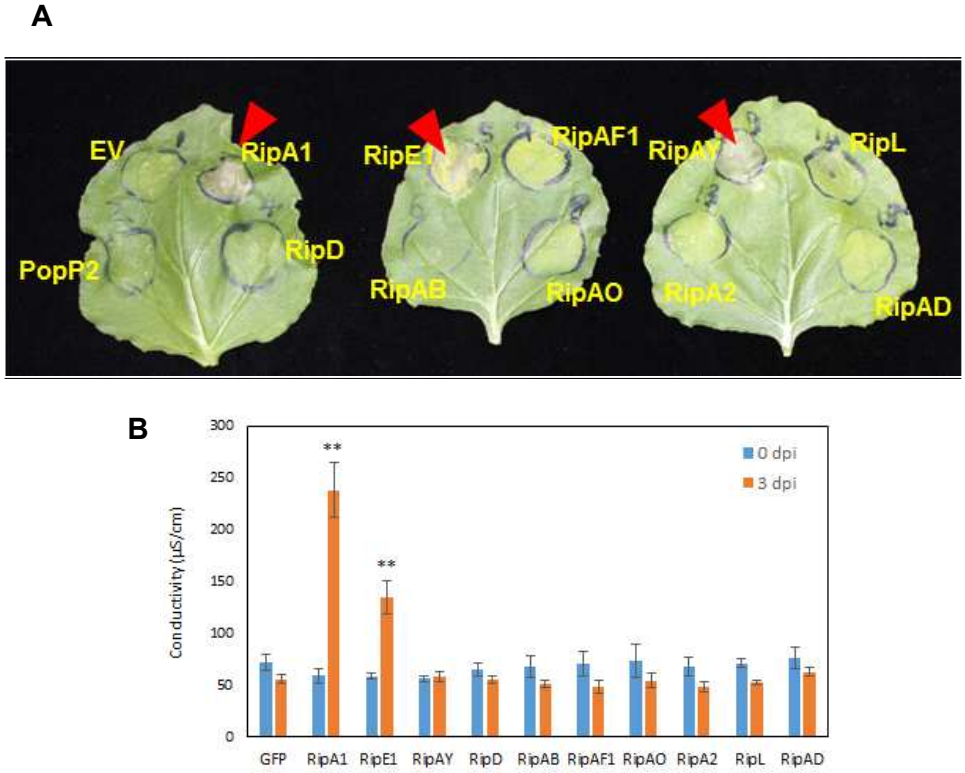

Figure 2. Several NLS-containing effectors trigger HR-like cell death in *N. benthamiana*

(A) Analysis of cell death induction by effectors. *N. benthamiana* plants were infiltrated with *A. tumefaciens* AGL1 strains carrying each effector construct, the empty vector (EV), or PopP2 as controls for the transient expression. The photographs were taken at 9 days post infiltration (9 dpi). Red arrows indicate cell death (Results from Dr. Wanhui Kim). (B) Quantification of effector-triggered cell death. Electrolyte leakage was measured in *N. benthamiana* leaf discs transiently expressing *GFP* or each effector at 0 and 3 dpi. Error bars represent the standard error of the mean (SEM; n=8). Statistical significance compared to *GFP*-expressing leaf is indicated by asterisks (Student's t-test, **p<0.01). The results in (A) and (B) are representative of three independent experiments.

RipAD, RipD, and RipAF1 disturbed flg22-induced ROS production in *N. benthamiana*

To identify immuno-suppressive effectors, the effector collection was screened for the ability to suppress the PAMP-triggered ROS production. In *N. benthamiana*, flg22, a PAMP derived from bacterial flagellin, is perceived by the receptor FLS2 and upon perception, apoplastic ROS generation is triggered rapidly (Chinchilla et al., 2007; Hann and Rathjen, 2007; Segonzac et al., 2011). Leaf discs transiently expressing each effector were harvested at 1 dpi and treated with flg22 for the experiment. The results showed that two effectors, RipAD and RipD, suppressed the production of ROS (Figure 3A and 3C). Also *RipAF1*-expressing leaf discs exhibited delayed ROS burst, where the peak of ROS production appeared about 10 min later than in the *GFP*-expressing leaves (Figure 3A). However, total ROS production for 75 min in *RipAF1*-expressing leaves was not reduced (Figure 3C). These results indicate that RipAF1 interfered with flg22-triggered ROS production in a different way from how RipAD and RipD did.

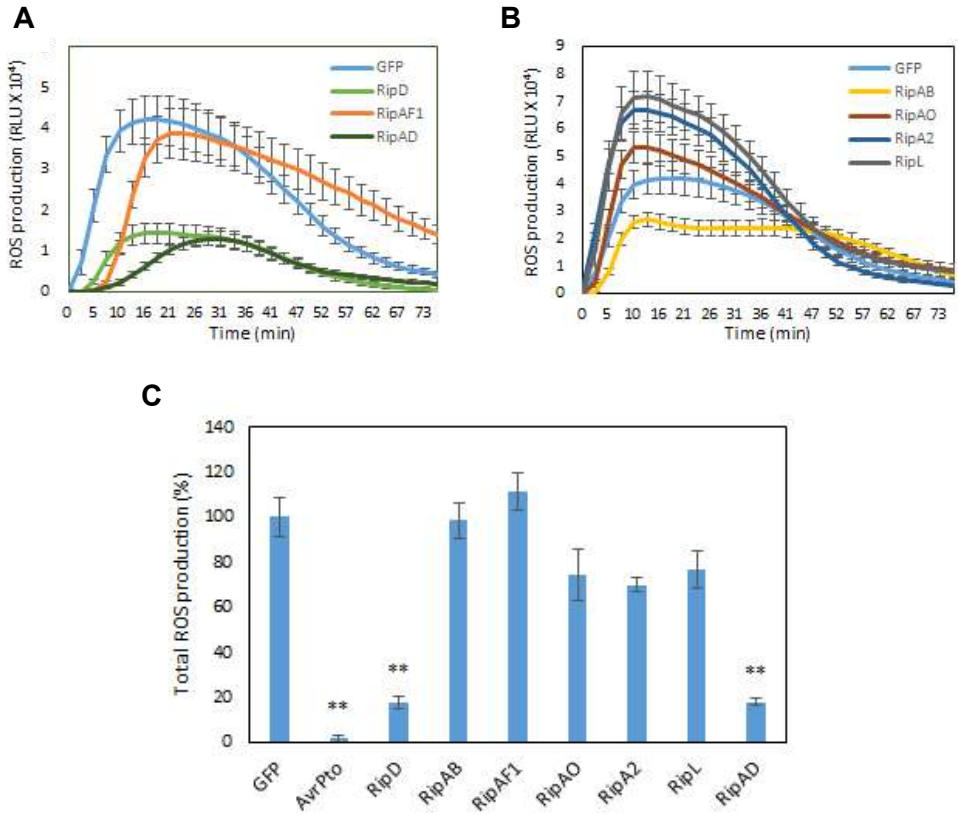

Figure 3. ROS burst in *N. benthamiana* expressing NLS-containing effectors

Flg22-induced ROS burst over time. (A) Three effectors that showed delayed (RipAF1) or suppressed (RipD and RipAD) ROS production compared to GFP were presented. (B) The other effectors that did not show delay or significant suppression of ROS production. (C) Total ROS production during 75 min after flg22 treatment. Data are presented as relative (%) to GFP control and AvrPto was included as a positive control of ROS suppression. Data shown in (A-C) are means ± SEM (n=16) from one representative of three independent experiments. Statistical significance compared to *GFP*-expressing leaf is indicated by asterisks in (C) (Student's t-test, **p<0.01). RLU, relative light unit.

RipD, RipAO, and RipAD disturbed flg22-induced gene expression in *N. benthamiana*

The other early immune response induced by PAMP is defense-oriented transcriptional reprogramming (Navarro et al., 2004; Zipfel et al., 2004; Zipfel et al., 2006; Wan et al., 2008). Three marker genes, *NbCYP71D20*, *NbACRE31*, and *NbACRE132* were identified to be expressed within 30 min after elicitation (Heese et al., 2007; Segonzac et al., 2011; Le Roux et al., 2015). To examine the effect of the effectors on PAMP-induced transcriptional activation of defense genes, transcription of these three marker genes in *N. benthamiana* leaves expressing each effector was monitored by quantitative RT-PCR 1 h after flg22 treatment (Figure 4). PopP2 is a well-characterized *R. solanacearum* effector, which was shown to suppress the induction of *NbACRE132* (Le Roux et al., 2015). Therefore, PopP2 was included for the experiment as a control. It was found that PopP2 reduced induction of *NbCYP71D20* and *NbACRE132* (Figure 4A and 4C). Among the selected effectors, three effectors impaired the expression of *NbCYP71D20* as much as or more than PopP2 did (Figure 4A). RipD reduced induction of two genes, *NbCYP71D20* and *NbACRE31,* to about 30% and 60% of the GFP control, respectively (Figure 4A and 4B). None of the effectors impaired induction of all the three genes. This may be because induction of *NbACRE31* and *NbACRE132* was not enough to see the difference between control and effector-expressing samples, which will be further discussed later.

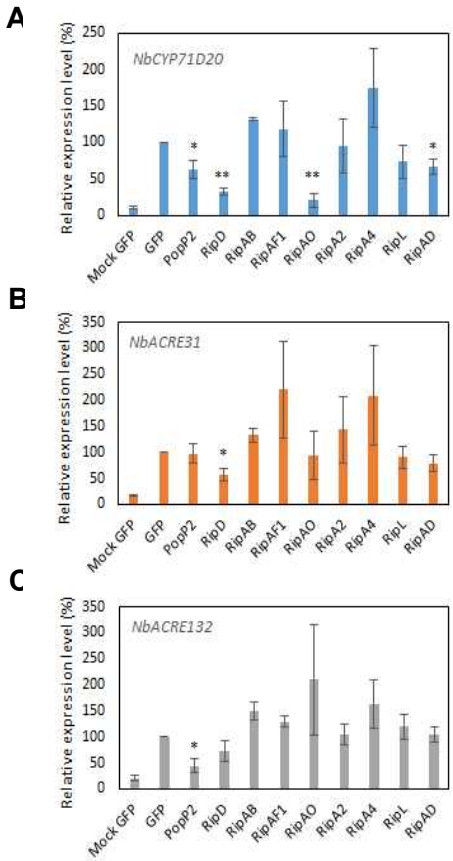

Figure 4. Flg22-induced marker gene expression in *N. benthamiana* expressing effectors

Induction of *NbCYP71D20* (A), *NbACRE31* (B) and *NbACRE132* (C) marker gene expression in *N. benthamiana* leaf transiently expressing GFP or each effector. Quantitative RT-PCR was conducted 60 min after flg22 treatment. Water-treated mock GFP was included as a negative control. All samples were normalized by *NbEF1α* and the data represent the ratio of expression levels (%) compared to the flg22-treated GFP sample. Error bars represent the SEM (n=3). Statistically significant expression compared to flg22-treated *GFP*-expressing leaf is indicated by asterisks (Student's t-test, *p<0.05, **P<0.01). Data are the means of three independent experiments.

Characterization of the effect of *Ralstonia solanacearum* NLS-containing type III effectors on immunity through constitutive expression in Arabidopsis

Obtention of *Arabidopsis* transgenic lines overexpressing NLS-containing effectors

Stable expression of effectors in every plant cells throughout the whole life could help find out on what cellular process or developmental stage effectors have an effect in a more visible manner. For this, transgenic *Arabidopsis* overexpressing each selected effector (Effector-expressing lines, EELs) were generated (Table 3). Col-0 plants were transformed with *A. tumefaciens* containing each effector constructs (*35S::Rip-3xFLAG*) using floral dip method (Clough and Bent, 1998). Then transformants were screened based on the kanamycin resistance associated with the transgenes. No primary transformants (T1) expressing *RipE1*, *RipAB*, *RipAF1*, and *RipAY* were recovered on selective medium containing kanamycin. Only one T1 seedling expressing *RipA1* was recovered but when transferred to soil, it did not survive. This could result from a deleterious effect of overexpression of these effectors, causing low transformation efficiency or death of the transformants. For RipA2, RipD, RipL, RipAD, and RipAO, T2 seeds descending from self-pollination of T1 plants were sown on the selective medium and seedlings following 3:1 (recovered: dead) segregation ratio were determined to contain single transgene in their T1 parents. Finally, T3 seeds were screened on the same medium and seedlings recovered

100% were selected as homozygous plants.

To confirm whether the effector transgenes are expressed in the T3 homozygous plants, RT-PCR analysis was conducted (Figure 5). Leaf tissues of all the T3 homozygous lines obtained were taken and frozen, and among them, two samples descending from each T1 line were chosen randomly for the analysis. When cDNA derived from the samples and WT was amplified with effector-specific primers, clear bands were observed except for sample 2, 39, 23, 26, and WT in the gel. PCR products from *RipAD*-expressing lines exhibited two bands with similar size caused by unspecific binding of the primers, resulting in the faint effector-specific bands. When the two bands were extracted and sequenced, one was proved to be from an *Arabidopsis* gene. Similarly, *RipAO*-specific primers amplified another *Arabidopsis* gene, causing a band in WT. Based on relative band size quantified using ImageJ, maximum three independent lines from different T1 lines were selected as final lines to be used for further characterization (Table 4). Also, effector expression in each final line was verified by sequencing the DNA extracted from the gel. These results indicate that effector transgenes are successfully expressed in *Arabidopsis* although expression of effector-FLAG fusion proteins needs to be confirmed by Western blotting.

Table 3. Obtention of EELs

Effector	Construct[a]	T1 lines transferred to soil	T2 with one insertion event[b]	T2 lines transferred to soil	T3 Homozygous line	Final line[c]
RipA1	CSG148	A1-1	-	-	-	-
RipA2	CSG158	A2-1 to 10	A2-7	A2-07-1 to 10	A2-7-6, 7, 10	oxA2-1 A2-7-6
RipD	CSG149	D-1 to 20	D-13, 17, 19, 20	D-13-1 to 05 D-17-1 to 10 D-19-1 to 10 D-20-1 to 10	D-13-1, 2, 3 D-17-1, 5 D-20-1, 5, 6	oxD-1 D-13-2 oxD-2 D-17-1 oxD-3 D-20-5
RipE1	CSG150	-	-	-	-	-
RipL	CSG159	L-1 to 24	L-8, 13, 14, 16, 17, 21	L-08-1 to 10 L-13-1 to 05 L-14-1 to 10 L-16-1 to 10 L-17-1 to 20 L-21-1 to 10	L-16-9	oxL-1 L-16-9
RipAB	CSG151	-	-	-	-	-
RipAD	CSG160	AD-1 to 14	AD-1, 03	AD-1-1 to 10 AD-3-1 to 10	AD-1-1, 3, 7, 8, 10	oxAD-1 AD-1-1
RipAF1	CSG152	-	-	-	-	-

Table 3. Obtention of EELs *(Continued)*

				AO-18-1 to 10	AO-18-1, 2, 7		
				AO-19-1 to 10	AO-19-5, 7	oxAO-1	AO-18-2
RipAO	CSG153	AO-1 to 23	AO-18, 19, 20, 21, 23	AO-20-1 to 10	AO-20-2, 4, 6	oxAO-2	AO-21-7
				AO-21-1 to 10	AO-21-7	oxAO-3	AO-23-8
				AO-23-1 to 10	AO-23-4, 6, 7, 8, 9		
RipAY	CSG154	-	-	-	-	-	

[a] Glycerol stock number of *A. tumefaciens* AGL1 carrying *35S::Rip-3xFLAG* constructs

[b] Selection of seedlings following 3:1 (recovered: dead) segregation on kanamycin medium

[c] Expression of each effector transgene were verified by RT-PCR and DNA sequencing (Figure 5 and table 3).

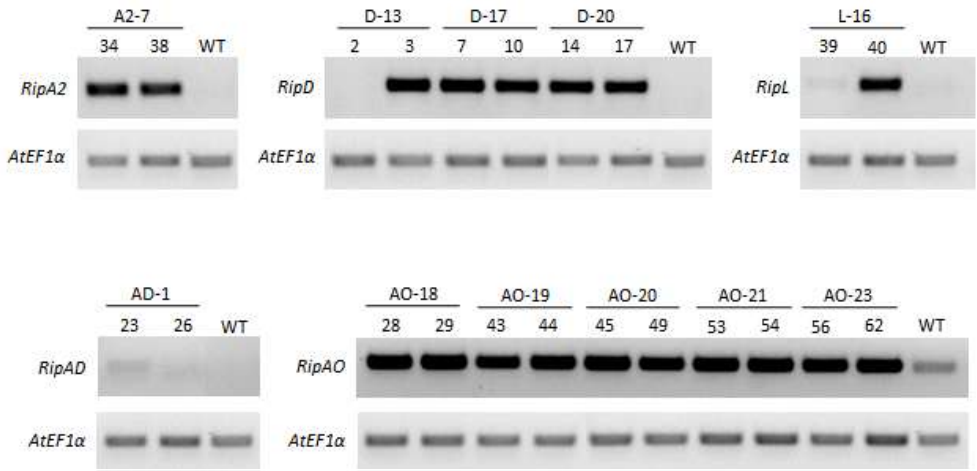

Figure 5. Transgene expression in effector transgenic *Arabidopsis* homozygous lines

RT-PCR analysis was carried out with cDNA derived from leaves of wild type Col-0 plant (WT) and T3 homozygous lines using each effector specific primer set. Among the leaf samples from all of the selected homozygous lines, two samples descending from different T1 lines were chosen randomly to confirm the transgene expression. *AtEF1α* gene was amplified as a control.

Table 4. Selection of final EELs

Sample Number	Line Name	Expression level[a]	Selected as a final line
34	A2-7-6	1.56	O
38	A2-7-10	1.12	
2	D-13-1	0.00	
3	D-13-2	1.30	O
7	D-17-1	0.81	O
10	D-17-5	1.06	
14	D-20-5	1.40	O
17	D-20-6	1.06	
18	L-16-9	0.03	
40	L-16-9	1.08	O
23	AD-1-1	0.03	O
26	AD-1-7	0.01	
28	AO-18-1	1.15	
29	AO-18-2	0.82	O
43	AO-19-5	1.26	
44	AO-19-7	1.27	
45	AO-20-2	0.86	
49	AO-20-4	1.31	
53	AO-21-7	0.74	O
54	AO-21-7	0.69	
56	AO-23-4	1.10	
62	AO-23-8	0.84	O

[a] Relative DNA band intensity on TAE agarose gel quantified using ImageJ

Preliminary characterization of PAMP-induced ROS production in EELs

To identify immuno-suppressive activity of effectors in *Arabidopsis,* PAMP-triggered ROS production and growth inhibition was examined in EELs. First, ROS burst assays were conducted in the same way as in *N. benthamiana* (Figure 6). Like in *N. benthamiana*, flg22 is recognized by the receptor FLS2 in *Arabidopsis* and thus flg22 was used as an elicitor (Gomez-Gomez and Boller, 2000; Chinchilla et al., 2006). *Arabidopsis* plants were sown on soil and grown under short-day (SD) light condition for the experiment. *RipD*-expressing lines could not germinate and grow well in the soil, and also the phenotypes of individuals in the same line was not homogenous. For these reasons, oxD-1, oxD-2, and oxD-3 were excluded from soil-based experiments. Leaf discs of the other EELs, WT, and *fls2* mutant were treated with 100nM flg22 and ROS burst was monitored (Figure 6A). In *fls2*, which lacks flg22 binding activity, almost no signal was detected. Contrary to the results from transient expression in *N. benthamiana*, none of the effectors suppressed ROS generation. This might be because the concentration of flg22 was not proper for *Arabidopsis*, resulting in saturated response and making it hard to observe intermediate levels of reduction. Therefore, elicitation by decreased concentration of flg22 (10 nM flg22) was next tested (Figure 6B). All of the tested EELs exhibited slightly reduced ROS production, but there was no significant difference from WT. Altogether, the effectors seem to act on the flg22-triggered immune response differently in *N. benthamiana* and *Arabidopsis.*

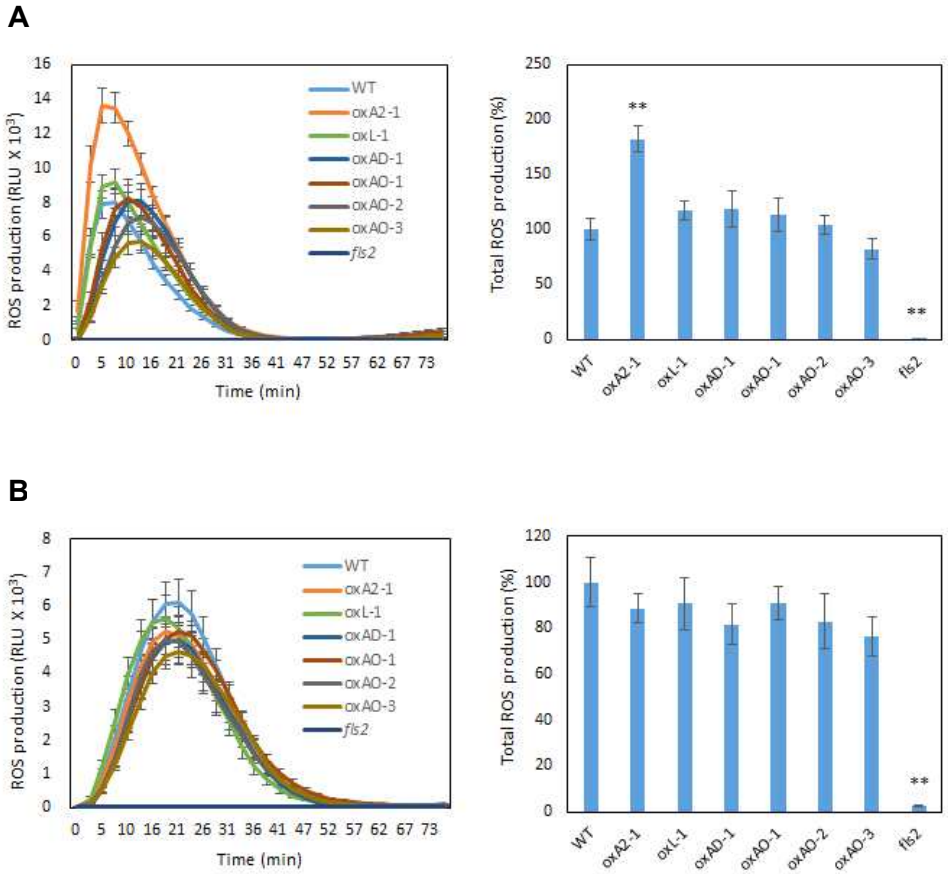

Figure 6. PAMP-triggered ROS burst in EELs

ROS burst induced by 100 nM flg22 (A) or 10 nM flg22 (B). ROS production over time and total ROS production during 75 min of elicitation were measured in leaf discs from WT, *fls2* mutant, and each EEL. Data are presented as relative (%) to WT. Error bars represent the SEM (n=16). Statistical significance compared to WT is indicated by asterisks (Student's t-test, **P<0.01).

Some of EELs showed reduced sensitivity to elf18-induced seedling growth inhibition

Prolonged treatments of PAMPs such as flg22 or elf18 result in seedling growth inhibition (SGI) of young seedlings, which is referred to as 'growth-defense tradeoff' (Gomez-Gomez et al., 1999; Zipfel et al., 2006; Huot et al., 2014). Although the exact molecular basis of this phenomenon is not clear yet, it indicates that plants balance resources allocated to growth and immunity to maintain optimal growth while at the same time ensuring immunity to pathogens (Malinovsky et al., 2014). To identify the effectors that suppress PTI via targeting this pathway, elf18-triggered SGI assay with all of the EELs, WT and *fls2 efr cerk1* triple mutant (*fec*) plants were carried out (Figure 7). As expected, elf18-treated WT seedlings, but not *fec* mutants, displayed significant reduction of fresh weight compared to untreated (0 nM) control. Although SGI was not completely blocked by effectors in EELs as was in *fec* plants, some of EELs showed reduced SGI compared to WT. While fresh weight of WT seedlings was reduced to about 50% and 25% of untreated control after treatment of 10 nM and 50 nM elf18, respectively, reduction ratio of oxD-1 was 65% and 40% under the same elf18 concentrations. Similary, oxAD-1 and oxAO-2 showed reduced SGI by about 5% compared to WT with 50 nM of elf18 treatment, and growth of oxAO-3 was also 10% less inhibited than that of WT after 10 nM elf18 treatment. These results indicate that effector overexpression affects plant sensitivity to PAMP, suggesting an alteration of the PTI pathway that may occur at any point from

PAMP perception by the PRR at the plasma membrane to transcriptional reprogramming in the nucleus. This could also means that the effectors may target the resource allocation diverted towards defense as an efficient infection strategy for the pathogens.

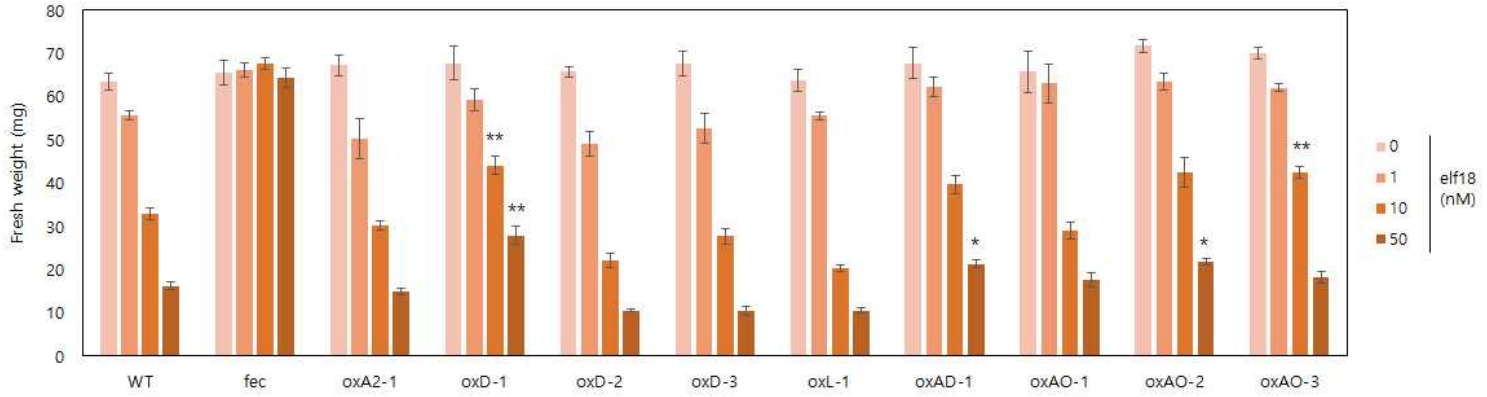

Figure 7. PAMP-triggered growth inhibition of *Arabidopsis* plants

Fresh weight of each EEL, WT and *fls2 efr cerk1* (*fec*) triple mutant seedlings grown for 9 days in MS containing increasing concentrations of elf18. Data are means ± SEM (n=6). Statistically significant difference compared to each WT treated with the same concentration of elf18 is indicated by asterisks (Student's t-test, *P<0.05, **P<0.01).

Preliminary morphological and physiological characterization of the EELs

Some of EELs exhibited disturbed root elongation and lateral root development

R. solanacearum is a soil-borne pathogen that infects through the roots (Peeters et al., 2013). Infection of *R. solanacearum* was shown to manipulate root architecture in petunia and *Arabidopsis* (Zolobowska and Van Gijsegem, 2006; Lu et al., 2018). Therefore, whether the selected effectors could disturb root growth and architecture was investigated by root growth assays with EELs. Seeds of WT and each EEL including *RipD*-expressing lines were sown on vertical MS plates and primary root (PR) length and number of lateral roots (LRs) were measured at 13 days after sowing (das) (Figure 8A and 8B). Most EELs exhibited shorter root length and less lateral roots than WT. These mild reductions found in the EELs except for *RipD*-expressing lines seem to have been caused by slightly slower germination (about 12 h) of them than that of WT, which made EELs start root growth later than WT (data not shown). But when it comes to oxD-2 and oxD-3, delay of germination was too long to be ignored. It took one to two more days for 80% of oxD-2 and oxD-3 seeds to germinate. This caused imprecise measurement of their root phenotype. But apart from the germination problem, oxD-2 and oxD-3 showed disturbed root morphology clearly (Figure 8C). They lacked LRs compared to WT and the other EELs. Also some of them had

LRs as long as PRs, making it hard to distinguish them. Therefore, it can be said that RipD disturbed root morphology, which suggests possible manipulation of hormonal pathways controlling root growth and development.

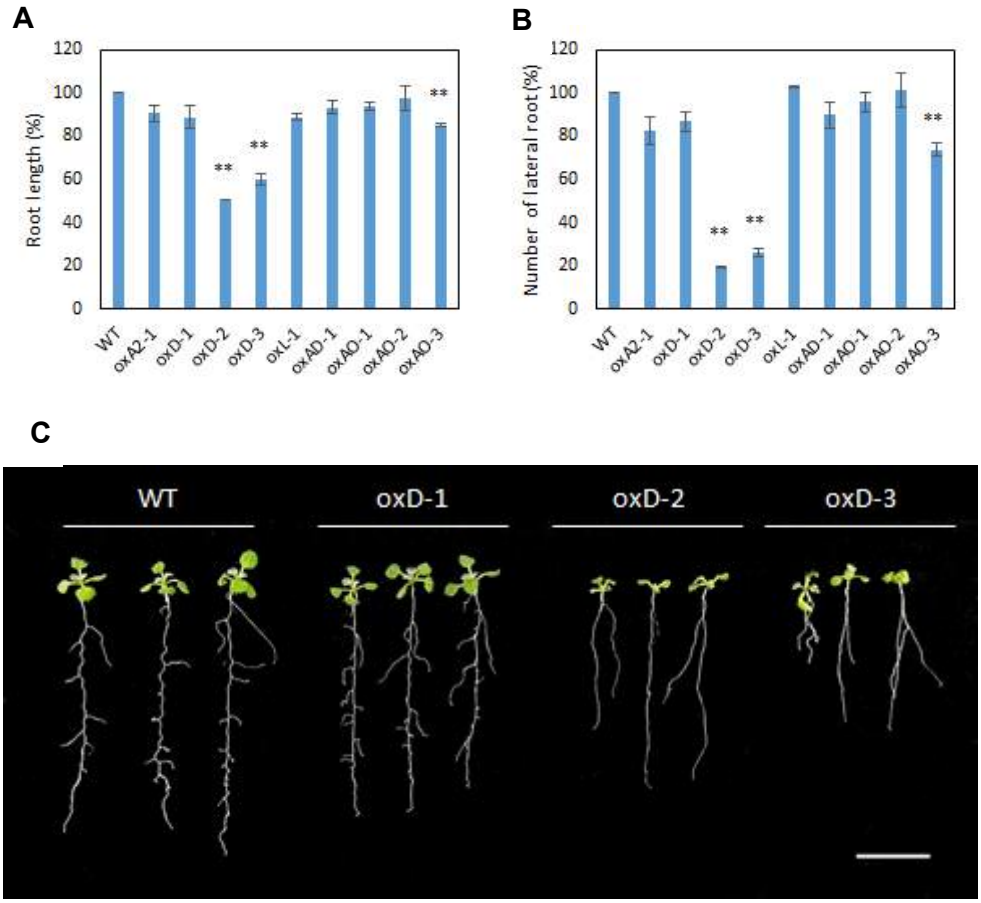

Figure 8. Phenotypic analysis of root growth of EELs

(A) Primary root length of EELs and wild type Col-0 (WT). (B) Number of lateral roots of EELs and WT. Both measurements in (A) and (B) were obtained via analyzing root images at 13 das using ImageJ. Data are means of two experiments ±SEM presented as relative (%) to WT. Five and ten seeds were sown on a plate for WT and each EEL, respectively. Statistical significance compared to WT is indicated by asterisks (Student's *t*-test, **p<0.01). (C) Root morphology of *RipD* transgenic lines and WT on MS medium. Photographs were taken at 13 day after seeding (das). Scale bars=10 mm.

RipD inhibited seed germination

After observing the delays of germination in *RipD*-expressing lines, seeds of each line were sown on MS plates for precise calculation of the phenotype (Figure 9A). Contrary to the WT and oxD-1 seeds, over 80% of which germinated in 2 days after sowing on MS, germination rate of oxD-2 and oxD-3 seeds was only about 75% and 60% at 4 das, respectively. It is well known that gibberellic acid (GA) and abscisic acid (ABA) play essential roles in regulating seed germination (Razem et al., 2006). GA breaks dormancy and stimulates germination by antagonistically suppressing ABA-triggered seed dormancy (Gubler et al., 2005; Graeber et al., 2012; Shu et al., 2016). Fluridone (FL) has been demonstrated to stimulate germination of a range of species including *Arabidopsis* via inhibiting ABA synthesis (Ali-Rachedi et al., 2004; Goggin and Powles, 2014). To find out the way to synchronize germination of transgenic seeds with WT, GA and FL treatment were tested (Figure 9B and 9C). Exogenous treatment of GA and FL did not to affect germination of non-dormant WT seeds, since WT seeds are already in optimal condition for the germination. Also, neither GA nor FL treatment could restore the germination capacity of *RipD* transgenic lines. Therefore, RipD interfered with seed germination of *Arabidopsis*, which was not mediated by disturbance of GA/ABA balance. Rather, RipD may disturb other hormonal pathways that regulate germination, perception of GA, or downstream signaling pathways such as induction of gene expression essential for the seeds to germinate. Further examination of the germination phenotype caused by RipD is required.

A

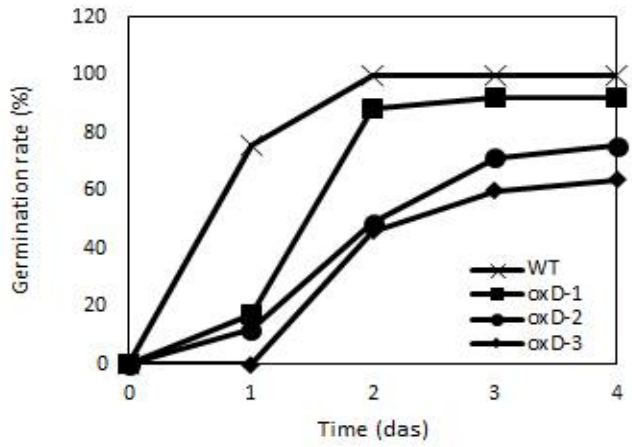
120
100
80
60
40
20
0
Germination rate (%)
0
1
2
3
4
Time (das)
WT
oxD-1
oxD-2
oxD-3

B

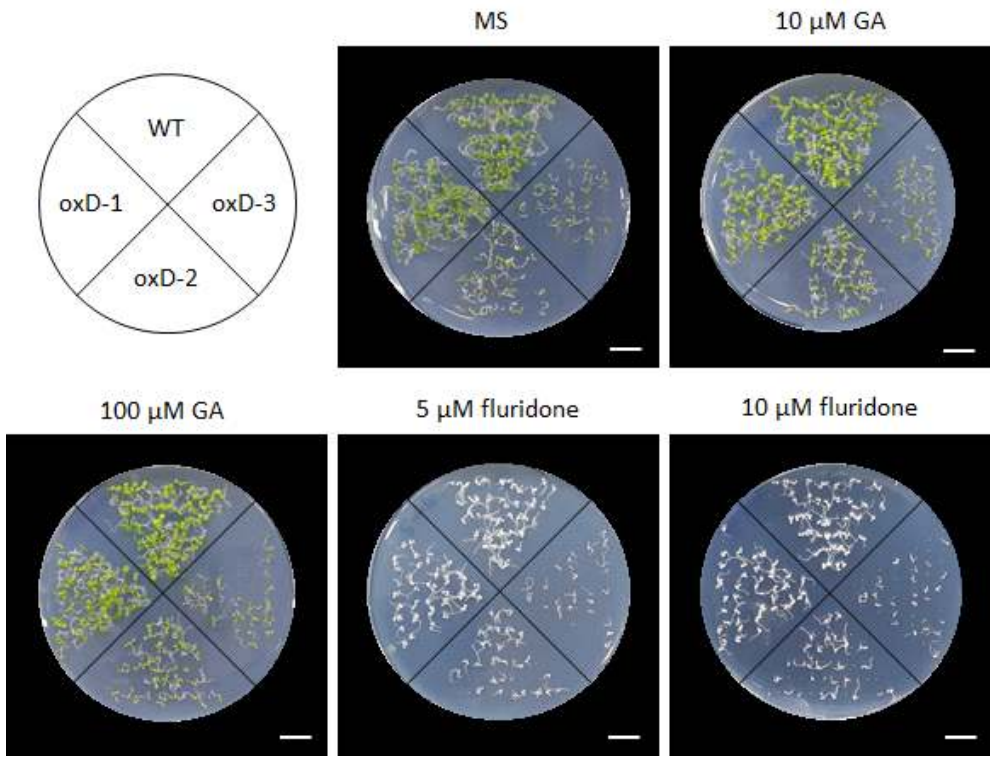
WT
oxD-1
oxD-3
oxD-2
MS
10 μM GA
100 μM GA
5 μM fluridone
10 μM fluridone

C

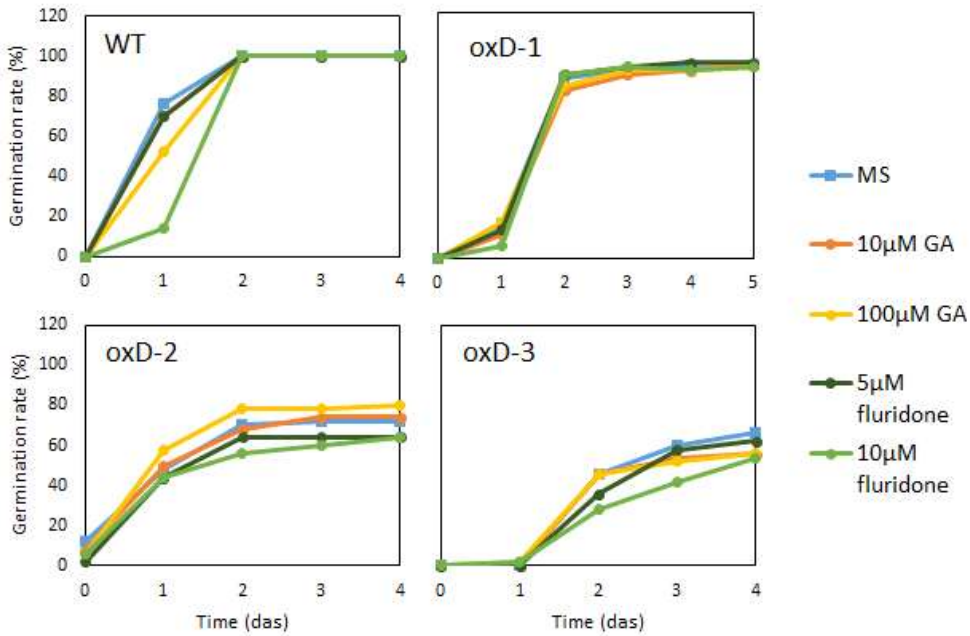

Figure 9. Germination phenotype of *RipD* transgenic seeds

(A) Germination rate of WT and *RipD* transgenic seeds in MS plates scored by radicle emergence. (B) Pictures showing the differences in germination of WT and *RipD* transgenic seeds in MS medium containing different concentrations of Gibberellic acid (GA) or fluridone. Photographs were taken 11 das. Scale bars=10 mm. (C) Germination rate of WT and *RipD* transgenic seeds in MS medium containing different concentrations of GA or fluridone scored by radicle emergence. 50 seeds were sown for each line.

EELs exhibited impaired germination and vegetative growth on soil

Phenotypic analysis of growth features over time is a key approach to understand and discover gene function (Boyes et al., 2001). To identify any morphological change caused by effectors during the entire life of plants, phenotypic data were measured from EELs grown on soil (Figure 10). As *Arabidopsis* is a facultative LD plant, growth of the plants is observed under LD in general. Under SD, flowering is delayed and plants favor vegetative growth, which enables longer and detailed observation of vegetative phase than under LD. Therefore, growth of EELs was observed under both SD and LD and recorded every 2 days. First, germination time of EELs on soil scored by emergence of green cotyledons was examined (Figure 10A). Germination of EELs was similar under SD and LD. Except for *RipL*- and *RipD*-expressing lines, germination rate of EELs was slightly lower than that of WT. OxL-1 showed more impaired germination, where the germination rate was about 80% and 90% under SD and LD, respectively. As mentioned before, *RipD*-expressing lines were severely impaired in germination and seedling establishment on soil. This observation corresponds to the disturbed root development and seed germination of *RipD*-expressing seeds on MS medium shown in Figure 8 and 9. On soil, where it is harder to acquire water and nutrients than on MS, the developmental defects of *RipD*-expressing lines caused much lower germination rate than on MS. About 90% of oxD-1 seeds germinated on MS, but only about 60% of them did on soil. And germination rate of oxD-2 and oxD-3 declined by more than 60% compared to on MS. Even after

germination, most seedlings failed to survive and grow. This indicates that impaired root development resulted in death of *RipD* transgenic seedlings.

To observe leaf development of EELs after germination, 8 plants of each EEL except for *RipD*-expressing lines and WT were transferred to pot tray at 12 das. Upon transfer, pictures of plants were taken every 2 days and analyzed using Rosette Tracker software to measure total leaf area and maximum rosette diameter (Figure 10B and 10C). The measurements continued until the image analysis got impossible because overlapping leaves made incorrect segmentation of individual plants under SD (at 32 das), or until WT started to produce the first flower bud under LD (at 18 das). Under both SD and LD condition, all the examined EELs exhibited slower and impaired leaf growth compared to WT plants. Contrary to the other EELs, which had developmental alteration to a similar degree, oxL-1 showed the highest level of alteration. The maximal alteration was observed in SD condition, where total leaf area and rosette diameter of oxL-1 plants at 32 das were only 8% and 25% of those measured in WT, respectively. Also under LD, oxL-1 exhibited the most impaired vegetative growth among EELs, whose total leaf area and rosette diameter were about 40% and 60% smaller than those of WT, respectively. Taken together, expression of the effectors, especially RipL, disturbed vegetative growth of *Arabidopsis*.

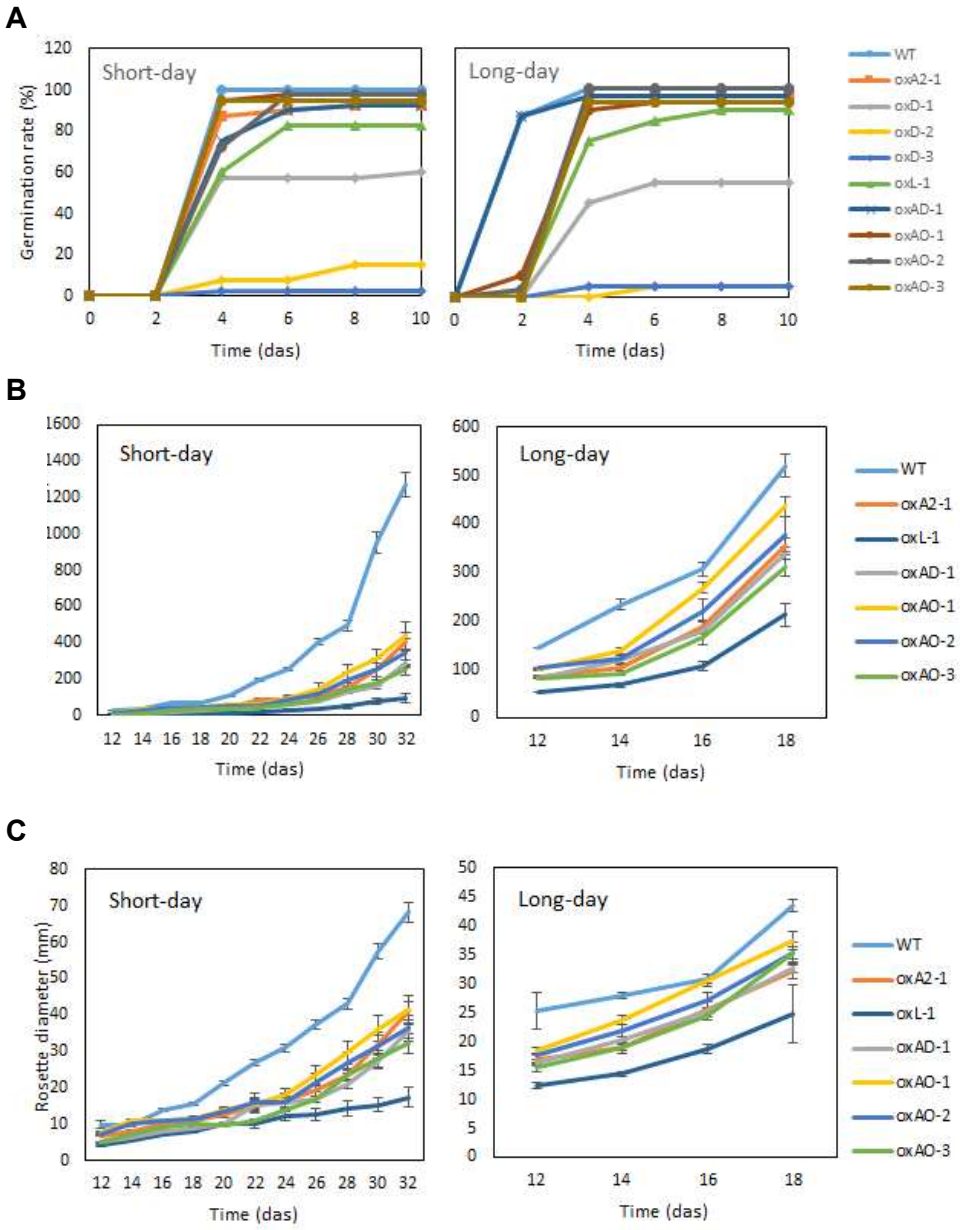

Figure 10. Comparison of developmental phenotype between WT and EELs in soil

(A) Germination rate of WT and effector transgenic seeds in soil scored by

cotyledon emergence under short-day or long-day condition. More than 30 seeds were sown for each line. (B) Total leaf area and (C) maximum rosette diameter of WT Col-0 and EELs under short-day or long-day condition. Data in (B) and (C) represent averages of 8 plants ±SEM measured via analyzing images of the plants using Rosette tracker.

DISCUSSION

Overexpression of effectors is an efficient experimental strategy, which helps to reveal target processes that cannot be found through loss-of-function analysis (Le Fevre et al., 2015). In this study, effectors containing putative NLS in their protein sequences were overexpressed in planta as molecular probes. To predict the presence of NLS in the effectors, two prediction algorythms – NLStradamus and cNLS mapper- were used and 25% of the examined effector sequences were predicted to carry NLS (Table 2). These two models use different methods and approaches. NLStradamus analyses frequency of basic residues such as arginine and lysine (Nguyen Ba et al., 2009). Meanwhile, cNLS mapper scores contributions of different amino acids at each position within an NLS class from activity-based profiles derived from systematic amino acid replacement analyses in budding yeast (Kosugi et al., 2009; Hari et al., 2017). Although they have proven to predict NLSs more accurately than traditional models used before, still there are some limitations. Firstly, they were generated by data from yeast, thus prediction for plants may be less effective although nuclear import pathways are highly conserved in eukaryotes. Secondly, the structural context of a native protein is not considered. Despite these problems, when the YFP-tagged effectors were transiently expressed in *N. benthamiana*, 4 effectors out of 10 were shown to be localized to the nucleus. Although more experiments are required to confirm the localization of the effectors, these prediction models seem to be useful

tools considering their simplicity and relatively high accuracy.

The NLS-containing effectors were analyzed for their impact on the immune system of *N. benthamiana*. Among the 10 selected effectors, three induced HR-like cell death (Figure 2). Plant cell death is associated with effector recognition in resistant plants as well as with the formation of lesions in susceptible plants (Alfano and Collmer, 2004). Knocking down of general ETI-regulators using virus-induced gene silencing (VIGS) would help to discriminate whether the cell death phenotype is caused by effector recognition by NB-LRR proteins or by toxicity of effectors (Choi et al., 2017; Gimenez-Ibanez et al., 2018). For example, *NbSgt1* is often required for NB-LRR protein functions by helping proper folding. Thus, if silencing of this gene compromises the cell death, it can be suggested that the cell death is due to recognition by *R* gene. On the other hand, there are effectors that trigger necrotrophic cell death such as Crinkler (CRN) effectors from oomycetes pathogens and PtrToxA effector produced by *Pyrenophora tritici-repentis* (Ciuffetti et al., 2010; Schornack et al., 2010; Toruno et al., 2016). However, since these examples are from necrotrophic pathogens, it is more likely that the cell death induced by effectors from *R. solanacearum*, which is hemi-biotrophic, is related to HR rather than necrosis.

Many effectors have been identified to suppress PTI responses (Macho and Zipfel, 2015). Here, the ability of effectors to interfere with PTI at different times and points in the early signaling pathways were analyzed. RipD, RipAD, and RipAF1 were shown to disturb flg22-triggered ROS production when transiently expressed in *N.*

benthamiana (Figure 3). RipAF1 did not reduce total ROS production compared to control, not like RipD and RipAD did, but it caused delayed ROS production. Notably, search for the functional domain revealed that RipAF1 is putative ADP-ribosyltransferase. Recent studies show that protein ADP-ribosylation plays important role in diverse cellular processes and is exploited by bacteria to dampen immunity (Feng et al., 2016). Interestingly, the T3E HopU1 from *Pseudomonas syringae* pv. *tomato* (*Pto*) DC3000, is an ADP-ribosyltransferase and modifies plant RNA binding protein GRP7 that bind mRNA encoding FLS2 and EFR (Fu et al., 2007; Jeong et al., 2011). This potentially contribute to the pathogen-induced translation of these mRNAs, resulting in reduced PRR levels (Nicaise et al., 2013). Therefore, RipAF1 may use similar strategy to interrupt and delay ROS production. Checking the *FLS2* transcript accumulation in *RipAF1*-expressing tissue could be the start to verify this hypothesis.

RipAD and RipD impaired ROS burst and also at least one defense gene expression (Figure 3 and 4). This suggests that they block early events in the signaling pathway at the receptor level. Or it is possible that they have multiple targets as many effectors do. For example, HopF2, another *Pto* DC3000 T3E, targets BAK1, MAPK cascade, and RIN4, an important immune regulator, to suppress flg22-induced responses (Wang et al., 2010; Zhou et al., 2014). Additionally, RipD is one of the core effectors conserved in 10 out of the 11 RSSC genome sequences and it is shown to be under strong positive selection (Peeters et al., 2013; Deslandes and Genin, 2014). Taken together, RipD may be an important virulence factor

that can suppress plant defense responses efficiently. In comparison, RipAO, which impaired one marker gene expression, but not ROS production, may target only the nucleo/cytoplasmic branch of PTI such as MAPK cascade and/or WRKY transcription factors.

While disturbance of ROS production by RipAD and RipD was quite clear and reproducible, none of the effector reduced the expression of all three marker genes (Figure 4). Also, I could not get the consistent results with the same experiments in EELs (data not shown). This may be because expression level and the optimal time for the induction are different between the marker genes. Expression level of *NbCYP71D20* whose induction was reduced by RipAD, RipD, and RipAO, was always more than twice those of *NbACRE31* and *NbACRE132*. Therefore, it is likely that the expression level of *NbACRE31* and *NbACRE132* was not high enough to see the reduction caused by the effectors. To check the optimal time that the expression of these genes reach its peak is required for more accurate experiment.

To observe morphological changes of plants induced by the effectors, effector-overexpressing *Arabidopsis* transgenic lines, namely EELs, were generated. But 5 out of 10 effectors were failed to get the primary transformants (Table 3). This may be attributed to a deleterious effect of the effector expression in seed or embryo. To solve this problem, transformation with the effector constructs under the control of an inducible promoter or tissue-specific promoter will be set up. Also copy number and insertion site of effector transgene will be assessed by southern blot (Fletcher, 2014).

While some of the selected effectors were found to disturb PTI responses in *N. benthamiana*, these effectors could not impair any of the defense responses in the corresponding EELs (Figure 6). This seems to result from the difference between *N. benthamiana* and *Arabidopsis*. There are possibilities that the same effectors function differently in these two plants. For example, the expression level of transgenes, sub-cellular localization of the effectors, and/ or signaling components between PAMP receptors and Rhoh could be different. Also, the effector target may be present only in *N. benthamiana*, but not in *Arabidopsis*. Finally, there is only a draft genome available for *N. benthamiana* and it has almost no genetic diversity, so functional characterization of PTI components in this species is less detailed than for *Arabidopsis*. Therefore, it would be worth to apply different experimental conditions (different dose/ kind of PAMPs) to examine PAMP-induced responses in EELs.

Among the EELs, *RipD* transgenic lines exhibited most interesting phenotypes in germination and root development (Figure 8 and 9). Observing smaller seedlings of *RipD*-expressing lines from the germination assays, I hypothesized that seed germination was impaired or delayed by *RipD* expression, meaning reduced germination potential rather than suppression of germination. Whether GA or ABA-inhibitor improve the germination was tested, but the effect of the treatment was not observed. In conclusion, germination delay of *RipD*-expressing lines may not be related to ABA-induced dormancy or GA-induced dormancy break. However, the reason why some of the oxD-2 and oxD-3 seeds never germinate is still in question.

All the EELs grown on soil showed reduced growth compared to WT plants. This phenotype could be caused by inhibition of development by the effectors, but it should be considered that overexpression of effectors can lead to misleading results. Overexpression of bacterial virulence factor may affect general homeostasis by causing protein imbalances, promiscuous interaction, and regulation of pathways that are not associated with the function of the effector (Gimenez-Ibanez et al., 2018). Considering that all the lines are smaller than WT, it is also possible that reduced growth is a side-effect of transformation. Comparison with proper control transgenic line which overexpresses *FLAG-GFP* would help assess the impact of protein overexpression on *Arabidopsis* growth. In spite of this drawback, some meaningful results were obtained by using the overexpression approach. The next step would be to identify effector targets to reveal the molecular mechanism by which the effectors manipulate plant immunity and development.

REFERENCES

Alfano, J.R., and Collmer, A. (2004). Type III secretion system effector proteins: double agents in bacterial disease and plant defense. Annual Review of Phytopathology **42,** 385-414.

Ali-Rachedi, S., Bouinot, D., Wagner, M.H., Bonnet, M., Sotta, B., Grappin, P., and Jullien, M. (2004). Changes in endogenous abscisic acid levels during dormancy release and maintenance of mature seeds: studies with the Cape Verde Islands ecotype, the dormant model of *Arabidopsis thaliana.* Planta **219,** 479-488.

Angot, A., Peeters, N., Lechner, E., Vailleau, F., Baud, C., Gentzbittel, L., Sartorel, E., Genschik, P., Boucher, C., and Genin, S. (2006). *Ralstonia solanacearum* requires F-box-like domain-containing type III effectors to promote disease on several host plants. Proceedings of the National Academy of Sciences of the United States of America **103,** 14620-14625.

Blume, B., Nurnberger, T., Nass, N., and Scheel, D. (2000). Receptor-mediated increase in cytoplasmic free calcium required for activation of pathogen defense in parsley. The Plant Cell **12,** 1425-1440.

Boller, T., and Felix, G. (2009). A renaissance of elicitors: perception of microbe-associated molecular patterns and danger signals by pattern-recognition receptors. Annual Review of Plant Biology **60,** 379-406.

Boyes, D.C., Zayed, A.M., Ascenzi, R., McCaskill, A.J., Hoffman, N.E., Davis, K.R., and Gorlach, J. (2001). Growth stage-based phenotypic analysis of Arabidopsis: a model for high throughput functional

genomics in plants. The Plant Cell **13,** 1499-1510.

Chinchilla, D., Bauer, Z., Regenass, M., Boller, T., and Felix, G. (2006). The Arabidopsis receptor kinase FLS2 binds flg22 and determines the specificity of flagellin perception. The Plant Cell **18,** 465-476.

Chinchilla, D., Zipfel, C., Robatzek, S., Kemmerling, B., Nurnberger, T., Jones, J.D., Felix, G., and Boller, T. (2007). A flagellin-induced complex of the receptor FLS2 and BAK1 initiates plant defence. Nature **448,** 497-500.

Choi, S., Jayaraman, J., Segonzac, C., Park, H.J., Park, H., Han, S.W., and Sohn, K.H. (2017). *Pseudomonas syringae* pv. *actinidiae* type III effectors localized at multiple cellular compartments activate or suppress innate immune responses in *Nicotiana benthamiana*. Frontiers in Plant Science **8,** 2157.

Ciuffetti, L.M., Manning, V.A., Pandelova, I., Betts, M.F., and Martinez, J.P. (2010). Host-selective toxins, Ptr ToxA and Ptr ToxB, as necrotrophic effectors in the P*yrenophora tritici-repentis*-wheat interaction. The New Phytologist **187,** 911-919.

Clough, S.J., and Bent, A.F. (1998). Floral dip: a simplified method for Agrobacterium-mediated transformation of *Arabidopsis thaliana*. The Plant Journal **16,** 735-743.

Coll, N.S., and Valls, M. (2013). Current knowledge on the *Ralstonia solanacearum* type III secretion system. Microbial Biotechnology **6,** 614-620.

Dagdas, Y.F., Belhaj, K., Maqbool, A., Chaparro-Garcia, A., Pandey, P., Petre, B., Tabassum, N., Cruz-Mireles, N., Hughes, R.K., Sklenar, J., Win, J., Menke, F., Findlay, K., Banfield, M.J., Kamoun, S., and Bozkurt, T.O. (2016). An effector of the Irish potato famine pathogen antagonizes a host autophagy cargo receptor. eLife **5**.

De Vylder, J., Vandenbussche, F., Hu, Y., Philips, W., and Van Der Straeten, D. (2012). Rosette tracker: an open source image analysis tool for automatic quantification of genotype effects. Plant Physiology **160,** 1149-1159.

Deslandes, L., and Rivas, S. (2011). The plant cell nucleus: a true arena for the fight between plants and pathogens. Plant Signaling & Behavior **6,** 42-48.

Deslandes, L., and Genin, S. (2014). Opening the *Ralstonia solanacearum* type III effector tool box: insights into host cell subversion mechanisms. Current Opinion in Plant Biology **20,** 110-117.

Feng, B., Liu, C., Shan, L., and He, P. (2016). Protein ADP-ribosylation takes control in plant-bacterium interactions. PLoS Pathogens **12,** e1005941.

Fu, Z.Q., Guo, M., Jeong, B.R., Tian, F., Elthon, T.E., Cerny, R.L., Staiger, D., and Alfano, J.R. (2007). A type III effector ADP-ribosylates RNA-binding proteins and quells plant immunity. Nature **447,** 284-288.

Fujiwara, S., Kawazoe, T., Ohnishi, K., Kitagawa, T., Popa, C., Valls, M., Genin, S., Nakamura, K., Kuramitsu, Y., Tanaka, N., and Tabuchi, M. (2016). RipAY, a plant pathogen effector protein, exhibits robust gamma-glutamyl cyclotransferase activity when stimulated by eukaryotic thioredoxins. The Journal of Biological Chemistry **291,** 6813-6830.

Genin, S. (2010). Molecular traits controlling host range and adaptation to plants in *Ralstonia solanacearum.* The New Phytologist **187,** 920-928.

Genin, S., and Denny, T.P. (2012). Pathogenomics of the *Ralstonia solanacearum* species complex. Annual Review of Phytopathology **50,**

67-89.

Gimenez-Ibanez, S., Hann, D.R., Chang, J.H., Segonzac, C., Boller, T., and Rathjen, J.P. (2018). Differential suppression of *Nicotiana benthamiana* innate immune responses by transiently expressed *Pseudomonas syringae* type III effectors. Frontiers in Plant Science **9,** 688.

Goggin, D.E., and Powles, S.B. (2014). Fluridone: a combination germination stimulant and herbicide for problem fields? Pest Management Science **70,** 1418-1424.

Gomez-Gomez, L., and Boller, T. (2000). FLS2: an LRR receptor-like kinase involved in the perception of the bacterial elicitor flagellin in Arabidopsis. Molecular Cell **5,** 1003-1011.

Gomez-Gomez, L., Felix, G., and Boller, T. (1999). A single locus determines sensitivity to bacterial flagellin in *Arabidopsis thaliana*. The Plant Journal **18,** 277-284.

Graeber, K., Nakabayashi, K., Miatton, E., Leubner-Metzger, G., and Soppe, W.J. (2012). Molecular mechanisms of seed dormancy. Plant, Cell & Environment **35,** 1769-1786.

Gubler, F., Millar, A.A., and Jacobsen, J.V. (2005). Dormancy release, ABA and pre-harvest sprouting. Current Opinion in Plant Biology **8,** 183-187.

Hann, D.R., and Rathjen, J.P. (2007). Early events in the pathogenicity of *Pseudomonas syringae* on *Nicotiana benthamiana*. The Plant Journal **49,** 607-618.

Hari, P.S., Sridhar, T.S., and Kumar, R.P.J.J.o.M.M. (2017). NLScore: a novel quantitative algorithm based on 3 dimensional structural determinants to predict the probability of nuclear localization in proteins containing classical nuclear localization signals. Journal of

molecular modeling **23,** 258.

Heese, A., Hann, D.R., Gimenez-Ibanez, S., Jones, A.M., He, K., Li, J., Schroeder, J.I., Peck, S.C., and Rathjen, J.P. (2007). The receptor-like kinase SERK3/BAK1 is a central regulator of innate immunity in plants. Proceedings of the National Academy of Sciences of the United States of America **104,** 12217-12222.

Huot, B., Yao, J., Montgomery, B.L., and He, S.Y. (2014). Growth-defense tradeoffs in plants: a balancing act to optimize fitness. Molecular Plant **7,** 1267-1287.

Jeong, B.R., Lin, Y., Joe, A., Guo, M., Korneli, C., Yang, H., Wang, P., Yu, M., Cerny, R.L., Staiger, D., Alfano, J.R., and Xu, Y. (2011). Structure function analysis of an ADP-ribosyltransferase type III effector and its RNA-binding target in plant immunity. The Journal of Biological Chemistry **286,** 43272-43281.

Jones, J.D., and Dangl, J.L. (2006). The plant immune system. Nature **444,** 323-329.

Kadota, Y., Shirasu, K., and Zipfel, C. (2015). Regulation of the NADPH oxidase RBOHD during plant immunity. Plant & Cell Physiology **56,** 1472-1480.

Kosugi, S., Hasebe, M., Tomita, M., and Yanagawa, H. (2009). Systematic identification of cell cycle-dependent yeast nucleocytoplasmic shuttling proteins by prediction of composite motifs. Proceedings of the National Academy of Sciences of the United States of America **106,** 10171-10176.

Kunze, G., Zipfel, C., Robatzek, S., Niehaus, K., Boller, T., and Felix, G. (2004). The N terminus of bacterial elongation factor Tu elicits innate immunity in Arabidopsis plants. The Plant Cell **16,** 3496-3507.

Le Fevre, R., Evangelisti, E., Rey, T., and Schornack, S. (2015). Modulation

of host cell biology by plant pathogenic microbes. Annual Review of Cell and Developmental Biology **31,** 201-229.

Le Roux, C., Huet, G., Jauneau, A., Camborde, L., Tremousaygue, D., Kraut, A., Zhou, B., Levaillant, M., Adachi, H., Yoshioka, H., Raffaele, S., Berthome, R., Coute, Y., Parker, J.E., and Deslandes, L. (2015). A receptor pair with an integrated decoy converts pathogen disabling of transcription factors to immunity. Cell **161,** 1074-1088.

Lecourieux, D., Ranjeva, R., and Pugin, A. (2006). Calcium in Plant Defence-Signalling Pathways. The New Phytologist **171,** 249-269.

Lee, A.H., Middleton, M.A., Guttman, D.S., and Desveaux, D. (2013). Phytopathogen type III effectors as probes of biological systems. Microbial Biotechnology **6,** 230-240.

Lu, H., Lema, A.S., Planas-Marques, M., Alonso-Diaz, A., Valls, M., and Coll, N.S. (2018). Type III secretion-dependent and -independent phenotypes caused by *Ralstonia solanacearum* in Arabidopsis roots. Molecular Plant-Microbe Interactions **31,** 175-184.

Macho, A.P. (2016). Subversion of plant cellular functions by bacterial type-III effectors: beyond suppression of immunity. The New Phytologist **210,** 51-57.

Macho, A.P., and Zipfel, C. (2015). Targeting of plant pattern recognition receptor-triggered immunity by bacterial type-III secretion system effectors. Current Opinion in Microbiology **23,** 14-22.

Malinovsky, F.G., Batoux, M., Schwessinger, B., Youn, J.H., Stransfeld, L., Win, J., Kim, S.K., and Zipfel, C. (2014). Antagonistic regulation of growth and immunity by the Arabidopsis basic helix-loop-helix transcription factor homolog of brassinosteroid enhanced expression2 interacting with increased leaf inclination1 binding bHLH1. Plant Physiology **164,** 1443-1455.

Mansfield, J., Genin, S., Magori, S., Citovsky, V., Sriariyanum, M., Ronald, P., Dow, M., Verdier, V., Beer, S.V., Machado, M.A., Toth, I., Salmond, G., and Foster, G.D. (2012). Top 10 plant pathogenic bacteria in molecular plant pathology. Molecular Plant Pathology **13,** 614-629.

Moore, J.W., Loake, G.J., and Spoel, S.H. (2011). Transcription dynamics in plant immunity. The Plant Cell **23,** 2809-2820.

Mukaihara, T., Hatanaka, T., Nakano, M., and Oda, K. (2016). *Ralstonia solanacearum* type III effector RipAY is a glutathione-degrading enzyme that is activated by plant cytosolic thioredoxins and suppresses plant immunity. mBio **7,** e00359-00316.

Navarro, L., Zipfel, C., Rowland, O., Keller, I., Robatzek, S., Boller, T., and Jones, J.D.G. (2004). The transcriptional innate immune response to flg22. interplay and overlap with *Avr* gene-dependent defense responses and bacterial pathogenesis. Plant Physiology **135,** 1113-1128.

Nguyen Ba, A.N., Pogoutse, A., Provart, N., and Moses, A.M. (2009). NLStradamus: a simple hidden Markov model for nuclear localization signal prediction. BMC Bioinformatics **10,** 202.

Nicaise, V., Joe, A., Jeong, B.R., Korneli, C., Boutrot, F., Westedt, I., Staiger, D., Alfano, J.R., and Zipfel, C. (2013). Pseudomonas HopU1 modulates plant immune receptor levels by blocking the interaction of their mRNAs with GRP7. The EMBO Journal **32,** 701-712.

Nuhse, T.S., Bottrill, A.R., Jones, A.M., and Peck, S.C. (2007). Quantitative phosphoproteomic analysis of plasma membrane proteins reveals regulatory mechanisms of plant innate immune responses. The Plant Journal **51,** 931-940.

Peeters, N., Guidot, A., Vailleau, F., and Valls, M. (2013). R*alstonia*

solanacearum, a widespread bacterial plant pathogen in the post-genomic era. Molecular Plant Pathology **14,** 651-662.

Poueymiro, M., and Genin, S. (2009). Secreted proteins from R*alstonia solanacearum*: a hundred tricks to kill a plant. Current Opinion in Microbiology **12,** 44-52.

Razem, F.A., Baron, K., and Hill, R.D. (2006). Turning on gibberellin and abscisic acid signaling. Current Opinion in Plant Biology **9,** 454-459.

Sang, Y., Wang, Y., Ni, H., Cazale, A.C., She, Y.M., Peeters, N., and Macho, A.P. (2018). The *Ralstonia solanacearum* type III effector RipAY targets plant redox regulators to suppress immune responses. Molecular Plant Pathology **19,** 129-142.

Sarris, P.F., Duxbury, Z., Huh, S.U., Ma, Y., Segonzac, C., Sklenar, J., Derbyshire, P., Cevik, V., Rallapalli, G., Saucet, S.B., Wirthmueller, L., Menke, F.L.H., Sohn, K.H., and Jones, J.D.G. (2015). A plant immune receptor detects pathogen effectors that target WRKY transcription factors. Cell **161,** 1089-1100.

Schornack, S., van Damme, M., Bozkurt, T.O., Cano, L.M., Smoker, M., Thines, M., Gaulin, E., Kamoun, S., and Huitema, E. (2010). Ancient class of translocated oomycete effectors targets the host nucleus. Proceedings of the National Academy of Sciences of the United States of America **107,** 17421-17426.

Segonzac, C., Feike, D., Gimenez-Ibanez, S., Hann, D.R., Zipfel, C., and Rathjen, J.P. (2011). Hierarchy and roles of pathogen-associated molecular pattern-induced responses in *Nicotiana benthamiana*. Plant Physiology **156,** 687-699.

Segonzac, C., Newman, T.E., Choi, S., Jayaraman, J., Choi, D.S., Jung, G.Y., Cho, H., Lee, Y.K., and Sohn, K.H. (2017). A conserved EAR motif is required for avirulence and stability of the *Ralstonia*

solanacearum effector PopP2 in planta. Frontiers in Plant Science **8,** 1330.

Shu, K., Liu, X.D., Xie, Q., and He, Z.H. (2016). Two faces of one seed: Hormonal regulation of dormancy and germination. Molecular Plant **9,** 34-45.

Sugio, A., Kingdom, H.N., MacLean, A.M., Grieve, V.M., and Hogenhout, S.A. (2011). Phytoplasma protein effector SAP11 enhances insect vector reproduction by manipulating plant development and defense hormone biosynthesis. Proceedings of the National Academy of Sciences of the United States of America **108,** E1254-1263.

Torres, M.A. (2010). ROS in biotic interactions. Physiologia Plantarum **138,** 414-429.

Torres, M.A., Dangl, J.L., and Jones, J.D.G. (2002). Arabidopsis gp91 ^{phox} homologues *AtrbohD* and *AtrbohF* are required for accumulation of reactive oxygen intermediates in the plant defense response. Proceedings of the National Academy of Sciences **99,** 517-522.

Toruno, T.Y., Stergiopoulos, I., and Coaker, G. (2016). Plant-pathogen effectors: cellular probes interfering with plant defenses in spatial and temporal manners. Annual Review of Phytopathology **54,** 419-441.

Valls, M., Genin, S., and Boucher, C. (2006). Integrated regulation of the type III secretion system and other virulence determinants in *Ralstonia solanacearum.* PLoS Pathogens **2,** e82.

Wan, J., Zhang, X.C., Neece, D., Ramonell, K.M., Clough, S., Kim, S.Y., Stacey, M.G., and Stacey, G. (2008). A LysM receptor-like kinase plays a critical role in chitin signaling and fungal resistance in Arabidopsis. The Plant Cell **20,** 471-481.

Wang, Y., Li, J., Hou, S., Wang, X., Li, Y., Ren, D., Chen, S., Tang, X., and Zhou, J.M. (2010). A *Pseudomonas syringae* ADP-ribosyltransferase

inhibits Arabidopsis mitogen-activated protein kinase kinases. The Plant Cell **22,** 2033-2044.

Zhang, J., Shao, F., Li, Y., Cui, H., Chen, L., Li, H., Zou, Y., Long, C., Lan, L., Chai, J., Chen, S., Tang, X., and Zhou, J.M. (2007). A *Pseudomonas syringae* effector inactivates MAPKs to suppress PAMP-induced immunity in plants. Cell Host & Microbe **1,** 175-185.

Zhou, J., Wu, S., Chen, X., Liu, C., Sheen, J., Shan, L., and He, P. (2014). The *Pseudomonas syringae* effector HopF2 suppresses Arabidopsis immunity by targeting BAK1. The Plant Journal **7,** 235-245.

Zipfel, C., Robatzek, S., Navarro, L., Oakeley, E.J., Jones, J.D., Felix, G., and Boller, T. (2004). Bacterial disease resistance in Arabidopsis through flagellin perception. Nature **428,** 764-767.

Zipfel, C., Kunze, G., Chinchilla, D., Caniard, A., Jones, J.D., Boller, T., and Felix, G. (2006). Perception of the bacterial PAMP EF-Tu by the receptor EFR restricts Agrobacterium-mediated transformation. Cell **125,** 749-760.

Zolobowska, L., and Van Gijsegem, F. (2006). Induction of lateral root structure formation on petunia roots: A novel effect of GMI1000 *Ralstonia solanacearum* infection impaired in *Hrp* mutants. Molecular Plant-Microbe Interactions **19,** 597-606.

초 록

*Ralstonia solanacearum*은 토양을 통해 전염되는 병원균으로 광범위한 식량 작물들에 풋마름병을 일으킨다. 이 병원균의 병원성은 기주의 세포 내로 이펙터 (type III effector, T3E) 단백질을 직접 주입하는 type III secretion system (T3SS)을 매개로 한다. T3E는 세균의 감염을 촉진하기 위해 식물의 면역 뿐만 아니라, 다양한 기주의 세포 과정들을 조절한다. 그러나 *R. solanacearum*의 T3E 구성의 복잡성 때문에, 그들이 어떻게 작용하는 지는 아직 잘 규명되지 않았다. 본 연구에서는 이펙터들이 식물에 미치는 영향을 알아내기 위해, 핵 위치 신호 서열을 가지는 것으로 추정되는 *R. solanacearum*의 T3E들을 각각 담배(*Nicotiana benthamiana*)와 애기장대(*Arabidopsis thaliana*)에 발현시켰다. 이펙터를 담배에서 일시적으로 발현 시킴으로써 (transient expression), 일부 이펙터들이 세포 사멸(cell death)을 유도하고 또 다른 이펙터들은 pattern-triggered immunity (PTI) 반응인 활성산소종(ROS) 생성과 뒤 이은 방어 관련 유전자들의 발현을 억제함이 밝혀졌다. 이펙터를 과다 발현하는 형질 전환 애기장대 식물체(EELs)를 생산하여 이들이 PTI를 억제할 수 있는지 또한 확인되었다. 마지막으로 EELs에서 이펙터들이 애기장대의 발달에 미치는 영향을 분석한 결과, 선별된 이펙터들 중 하나인 RipD가 종자 발아와 뿌리 발달을 방해함이 밝혀졌다. 면역 시스템과 뿌리 발달에 영향을 주는 것으로 밝혀진 이펙터들은 그들의 분자적 타겟과 병원성에 대한 기여도를 구명하기 위해 이후 더 연구될 것이다.

주요어: *Ralstonia solanacearum,* 이펙터, 식물 면역, PTI, 담배 (*Nicotiana benthamiana*), 애기장대 (*Arabidopsis thaliana*), 식물 발달

학번: 2017-21031